Rare Metal Materials and Engineering
Volume 51, Issue 3, March 2022
Available online at www.rmme.ac.cn

Science Press

Cite this article as: Li Hangyu, Wang Xianhui, Gao Qianwen, et al. Arc Erosion Behavior of Ag-TiB_2 Contact Materials with Ag Powders of Different Sizes[J]. Rare Metal Materials and Engineering, 2022, 51(03): 765-771.

ARTICLE

Arc Erosion Behavior of Ag-TiB_2 Contact Materials with Ag Powders of Different Sizes

Li Hangyu[1], Wang Xianhui[1], Gao Qianwen[1], Liang Yan[1,2], Fei Yuan[1]

[1] Shaanxi Key Laboratory of Electrical Materials and Infiltration Technology, Xi'an University of Technology, Xi'an 710048, China; [2] Northwest Institute of Nonferrous Metals, Xi'an 710016, China

Abstract: The Ag-TiB_2 contact materials with Ag powders of different sizes were prepared by spark plasma sintering. The relative density, electroconductivity, and hardness of Ag-4wt% TiB_2 contact materials were measured, and the arc erosion behavior of the contact materials was analyzed under the vacuum condition. The surface morphologies of Ag-4wt% TiB_2 contact materials after arc erosion were characterized by the scanning electron microscope. The arc duration was determined by the discharged waveform recorded by a Tektronix TDS-2014 dual channel digital memory oscilloscope, and the arc erosion mechanism was discussed. The results show that the relative density, electroconductivity, and hardness of Ag-4wt% TiB_2 contact materials are increased with decreasing the Ag powder size. Furthermore, the Ag-4wt% TiB_2 contact materials prepared from fine Ag powder have longer arc duration, larger erosion area, and shallower erosion pit, suggesting that the fine Ag powder is beneficial for arc dispersion and the improvement in arc erosion resistance.

Key words: contact material; Ag-TiB_2; Ag powder size; arc erosion

Due to its excellent arc erosion resistance, welding resistance, and environmentally benign characteristic, $AgSnO_2$ contact material is a desired substitute for AgCdO contact material in the low-voltage electrical apparatus[1-4]. However, the $AgSnO_2$ contact material presents large contact resistance and great temperature rise during long time service due to accumulation of insulative SnO_2 on the contact surface[5,6]. Therefore, TiB_2 ceramics with good electroconductibility and thermal conductivity are investigated to strengthen the Ag matrix, and the Ag-TiB_2 contact material was fabricated[7].

The arc erosion behavior of contact materials has been widely studied. Lungu et al[8] reported that the uniform structure is favorable for the improvement in the arc erosion resistance. Wang et al[9] demonstrated that the Ag-based contact nanocomposite is beneficial to arc dispersion and to the decrease in splash erosion. Xu et al[10] found that the fine SnO_2 particles can decrease the splash erosion due to larger viscosity of the molten pool of the $AgSnO_2$ contact material. Wang et al[11] found that the fine Al_2O_3 particles result in the shallower erosion pit in the Cu-Al_2O_3 composite. Zhang et al[12] reported that the fine SnO_2 particles can decrease the arc duration and the aggregation of strengthening particles in $AgSnO_2$ contact materials. The decrease in TiB_2 particle size can also improve the arc erosion behavior of Ag-TiB_2 contact material[13]. In fact, once the arc occurs, the arc extinction can reduce the arc erosion. In general, the second phase can promote the arc dispersion, which is beneficial to the arc extinction. The basic mechanism is that the arc is generated preferentially on the interface between Ag and the second phase. However, due to the complexity and instantaneity of arc, some problems of arc erosion behavior are still unclear. The effect of Ag powder size on the arc erosion behavior of Ag-TiB_2 contact material is rarely reported. In this research, the Ag-4wt% TiB_2 contact materials were fabricated with Ag powders of different sizes by powder metallurgy, the effect of Ag powder size on the properties of $AgTiB_2$ contact materials was studied, and the arc erosion behavior was discussed.

1 Experiment

The raw materials are Ag powder (purity of 99.9wt%;

Received date: March 08, 2021
Foundation item: National Natural Science Foundation of China (51971173); Doctoral Dissertation Innovation Fund of Xi'an University of Technology (310/252072011)
Corresponding author: Wang Xianhui, Ph. D., Professor, Shaanxi Key Laboratory of Electrical Materials and Infiltration Technology, Xi'an University of Technology, Xi'an 710048, P. R. China, Tel: 0086-29-82312185, E-mail: xhwang693@xaut.edu.cn

particle size of 72 and 0.4 μm) and TiB_2 powder (purity of 99.9wt%; particle size of 3 μm), and their morphologies are shown in Fig. 1. The Ag-TiB_2 powder with the mass ratio of Ag:TiB_2=96:4 was mixed at 200 r/min for 4 h and the ball-to-powder ratio was 40:1. The Ag-4wt% TiB_2 powder mixtures with Ag powders of 72 and 0.4 μm in size were named as Ag(72)-4wt% TiB_2 and Ag(0.4)-4wt% TiB_2, respectively. The ethyl alcohol and polyvinyl pyrrolidone (1wt%) were used as process control agent and dispersant, respectively. Fig.2 shows the morphologies of the powder mixture. Since Ag has good plasticity and toughness, some TiB_2 particles are embedded into the Ag powders. The powder mixture was sintered in a spark plasma sintering (SPS) furnace under the vacuum environment. The current, voltage, and temperature during sintering are shown in Fig.3. The heating rate was 30 °C/min, and the temperature of 450 and 650 °C was held for 5 min. The relative density was determined by Archimedes method. The hardness was tested on a HB-3000 Brinell hardness tester under a load of 250 kg and a steel ball with the diameter of 5 mm for 30 s. The electroconductivity was tested by a 7501-eddy electroconductivity gauge. All the values were the average of three measurements.

The vacuum arc erosion was tested on a modified TDR240A single crystal furnace. Each specimen mounted in a holder was used as a cathode, which moved vertically in the vacuum chamber. The anode was a pure tungsten needle with a radius of 5 mm and a tip radius of 1 mm. The gap distance and the voltage between anode and cathode was 2 mm and 3.0 kV, respectively. When the chamber was evacuated to 5.0×10^{-3} Pa, the anode moved downward at a speed of 0.2 mm/min until the electrical breakdown occurred. Each specimen was tested for 1 and 40 times, and the data of current waveforms were collected by the Tektronix TDS-2014 dual channel digital memory oscilloscope (200 MHz). The eroded surface morphologies were characterized by a TESCAN-Vega XMU 2 scanning electron microscope (SEM), and the erosion areas were calculated by the Image-Pro Plus 6.0 software.

2 Results and Discussion

2.1 Properties of Ag-TiB_2 contact materials

Table 1 shows the relative density, electroconductivity, and hardness of the Ag-4wt% TiB_2 contact materials prepared by Ag powders with different particle sizes. It can be seen that the relative density of the Ag(0.4)-4wt% TiB_2 contact material is 95.2%, which is increased by 1.82% compared with that of the Ag(72)-4wt% TiB_2 contact material. Similarly, compared with those of the Ag(72)-4wt% TiB_2 contact materials, the electroconductivity and hardness of Ag(0.4)-4wt% TiB_2 contact materials are increased by 10.07% and 28.55%, respectively.

According to the relative density results in Table 1, it can be concluded that large pores exist between the Ag powder of 72 μm in size and TiB_2 powder of 3 μm in size owing to the difference in geometry and size of the Ag and TiB_2 particles. The ultrafine Ag powders (0.4 μm) can fill the pores during sintering, thus increasing the relative density. Besides, based on the calculation in Ref.[14], the melting point of Ag powder of 72 and 0.4 μm in size is 961.6 and 922.0 °C, respectively, which is far above the sintering temperature. According to the Kelvin equation[15], the vapor pressure is increased with decreasing the particle size, and the plasma is much easier to generate for fine powder, thus increasing the diffusion effect and the mass transfer. Hence, the fine powder is beneficial to the sintering densification. Furthermore, based on the electroconductivity theory, the pores can increase the electron scattering, thus decreasing the electroconductivity. In addition, the high relative density is also beneficial for the high hardness.

2.2 Arc duration of Ag-TiB_2 contact materials

The variation and the related frequency distribution of arc duration of Ag-4wt% TiB_2 contact materials are shown in Fig. 4. As shown in Fig. 4a, the arc duration of Ag(72)-4wt% TiB_2 contact materials has a large fluctuation during the arc erosion for the first 20 times, and then is decreased during the arc erosion for the last 20 times. The similar tendency can also be observed for the Ag(0.4)-4wt% TiB_2 contact material, as shown in Fig. 4c. As shown in Fig. 4b, the Ag(72)-4wt% TiB_2 contact materials have an irregular distribution in arc duration, indicating that its arc duration has the overall large fluctuations, and the average arc duration is 16.62 ms with a standard deviation of 1.92 ms. However, for the Ag(0.4)-4wt% TiB_2 contact materials, the arc duration has a concentrated distribution, and the average arc duration is 17.21 ms with a standard deviation of 1.44 ms. Therefore, although Ag(0.4)-4wt% TiB_2 contact materials have larger average arc duration, their arc is much more stable than that of Ag(72)-

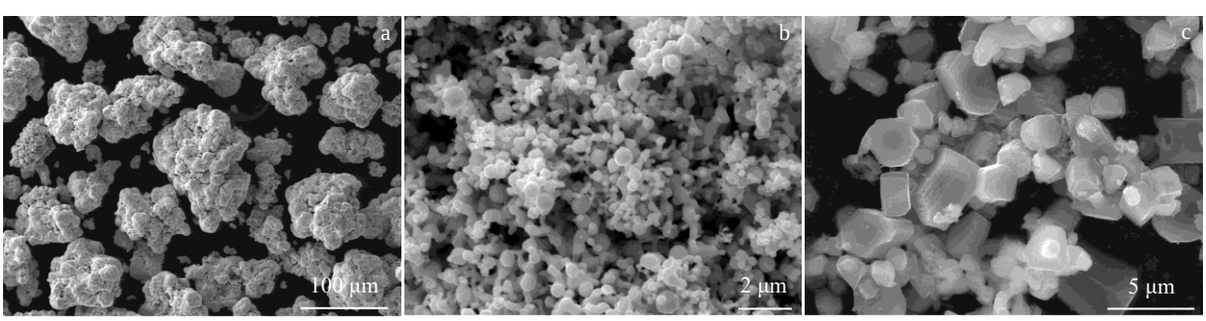

Fig.1 Morphologies of Ag powders with 72 μm (a) and 0.4 μm (b) in size and TiB_2 powder of 3 μm in size (c)

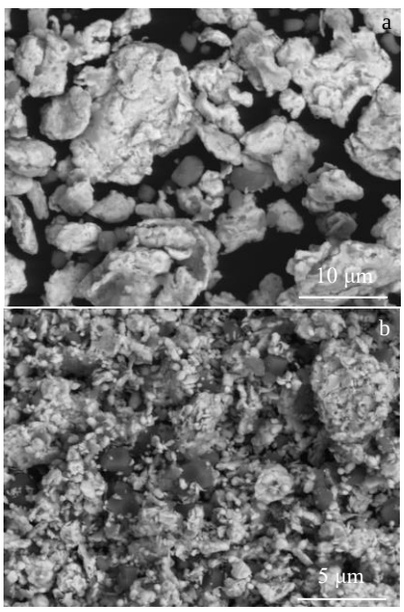

Fig.2 Morphologies of Ag-TiB_2 powder mixtures with different Ag powder sizes of 72 μm (a) and 0.4 μm (b)

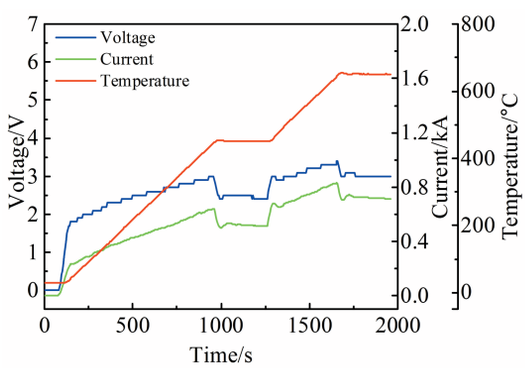

Fig.3 Current, voltage, and temperature during SPS sintering

Table 1 Properties of Ag-4wt% TiB_2 contact materials prepared from Ag powders with different sizes

Ag particle size/μm	Relative density/%	Electroconductivity/ %IACS	Hardness, HB/MPa
72	93.5	71.5	739
0.4	95.2	78.7	950

4wt% TiB_2 contact materials.

2.3 Eroded morphologies of Ag-TiB_2 contact materials after arc erosion for one time

Fig. 5 shows the eroded morphologies of Ag-4wt% TiB_2 contact materials after the first arc erosion. It can be seen that the Ag(0.4)-4wt% TiB_2 contact materials have larger erosion area than Ag(72) -4wt% TiB_2 contact materials do. The concentrated erosion pits appear with a discontinuous distribution for the Ag(72) -4wt% TiB_2 contact materials, suggesting that the arc hop occurs on the material surface. However, the smaller and shallower erosion pits appear on the surface of Ag(0.4) -4wt% TiB_2 contact materials. It is concluded that the fine Ag powders are beneficial for the arc dispersion, and the arc can move quickly on the surface of Ag-4wt% TiB_2 contact materials.

2.4 Eroded morphologies of Ag-TiB_2 contact materials after arc erosion for forty times

Fig. 6 shows the eroded surface morphologies of Ag-4wt%TiB_2 contact materials after arc erosion for 40 times. As shown in Fig. 6a, there is a relatively concentrated arc erosion of Ag(72)-4wt% TiB_2 contact materials, and the erosion area is 1.07 mm^2. The deep erosion pits and the flow traces can be found at the erosion center of Ag(72) -4wt% TiB_2 contact materials, as shown in Fig. 6b. However, the erosion pits of Ag(0.4) -4wt% TiB_2 contact materials are shallower and dispersedly distributed (Fig. 6d), and the erosion area reaches 2.13 mm^2. Hence, it can be concluded that the fine Ag powders are favorable for the arc dispersion and the improvement in arc erosion resistance.

2.5 Arc erosion mechanism

It is generally believed that the arc can be divided into gaseous ion arc and metallic ion arc[16,17], resulting in the material transfer between anode and cathode[18,19]. It is reported that the material characteristics, such as boiling point, work function, and particle size, can influence the arc characteristics, which further cause different material transfer behavior[20,21]. Once the vacuum breakdown eliminates the effects of gaseous ion, the arc is dominated by the metallic ion. Therefore, it is necessary to investigate the effects of Ag powder size and grain boundary on the electron emission in the cathode during arc erosion.

Fig. 7 shows the electron emission model at the boundary. Assuming that two Ag atoms exist at the boundary, an electron is restricted in the potential well. The lattice distortion occurs at the boundary, which affects the depth of the potential well. As a result, some of the electrons need less energy to escape from the metal surface. When the electric field reaches a certain value, the electron emission prefers to occur at the boundary.

The vapor layer exists at the metal surface, and the vapor pressure is increased with increasing the temperature, as shown in Fig. 8a. When the tungsten needle approaches the surface of Ag-TiB_2 contact materials, the electric field is increased, and the electron emission happens. On the one hand, the freedom electrons accelerated by the electric field collide with the Ag atoms, resulting in the ionization of Ag vapor. On the other hand, the thermal effect promotes the electron emission and even material evaporation, aggravating the ionization level. Consequently, the arc forms.

During this process, the Ag powder size can affect two aspects: the vapor pressure and the emission current. Based on the Kelvin equation[15], the saturation vapor pressure of Ag is increased with decreasing the radius, as expressed by Eq.(1):

$$\ln\frac{P_{Ag}(r)}{P_{Ag}(\infty)}=\frac{2\sigma V}{rRT} \quad (1)$$

where $P_{Ag}(r)$ is the saturation vapor pressure of Ag with the

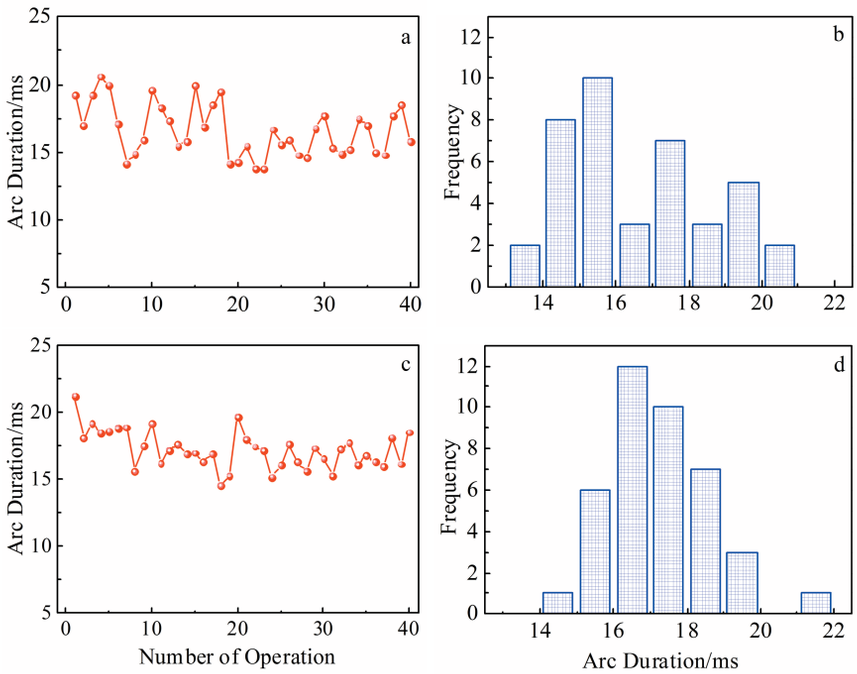

Fig.4 Arc duration (a, c) and its frequency (b, d) of Ag(72)-4wt% TiB_2 (a, b) and Ag(0.4)-4wt% TiB_2 (c, d) contact materials during arc erosion for 40 times

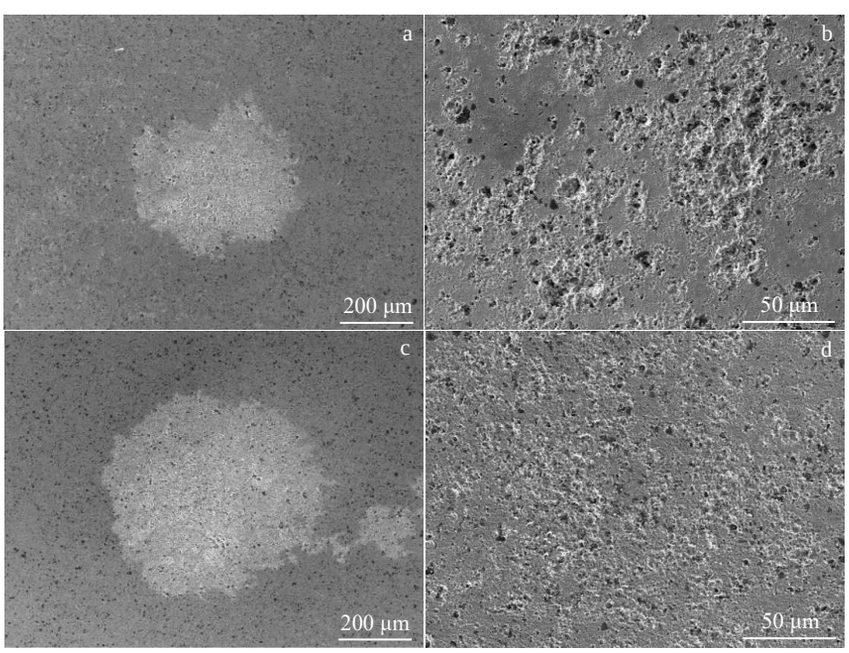

Fig.5 Eroded morphologies of Ag(72)-4wt% TiB_2 (a, b) and Ag(0.4)-4wt% TiB_2 (c, d) contact materials after arc erosion for one time

radius r; $P_{Ag}(\infty)$ represents the saturation vapor pressure of Ag with a flat surface, σ is the specific surface energy, V is the molar volume, R is the molar gas constant, and T represents the temperature.

Apparently, the fine Ag powders are beneficial for the large vapor pressure at metal surface, providing more ions to sustain the arc burning. Furthermore, the grain boundary has low energy barrier to emit electrons. Generally, the Ag-TiB_2 interface has the first priority to determine the electron emission spot[13]. The number and distribution of grain boundaries can subsequently influence the electron emission spot. For the Ag-TiB_2 contact materials, the distribution of TiB_2 no longer causes difference due to its unchanged particle size, and the number of grain boundaries of Ag(0.4) -4wt% TiB_2 contact materials is much larger than that of Ag(72) -4wt% TiB_2 contact materials (Fig. 8c and 8d). Therefore, the fine Ag

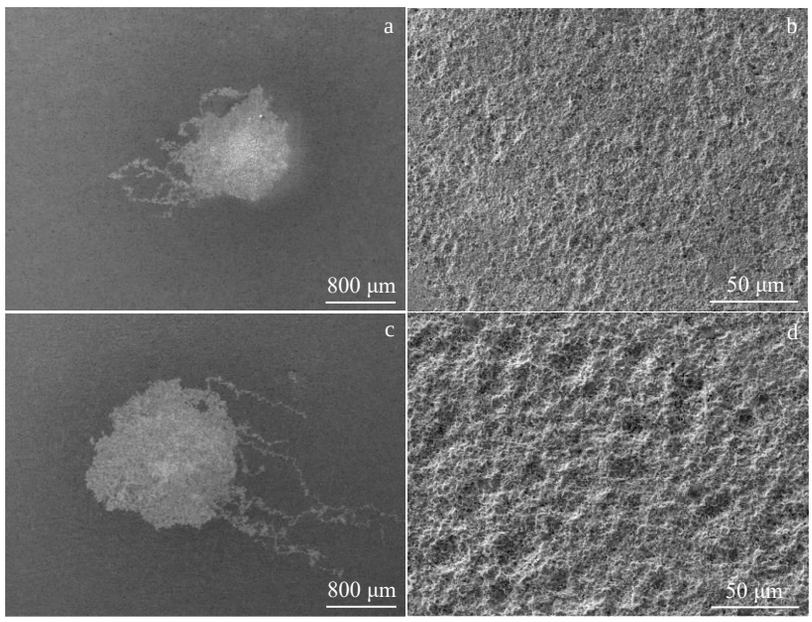

Fig.6 Eroded morphologies of Ag(72)-4wt% TiB_2 (a, b) and Ag(0.4)-4wt% TiB_2 (c, d) contact materials after arc erosion for 40 times

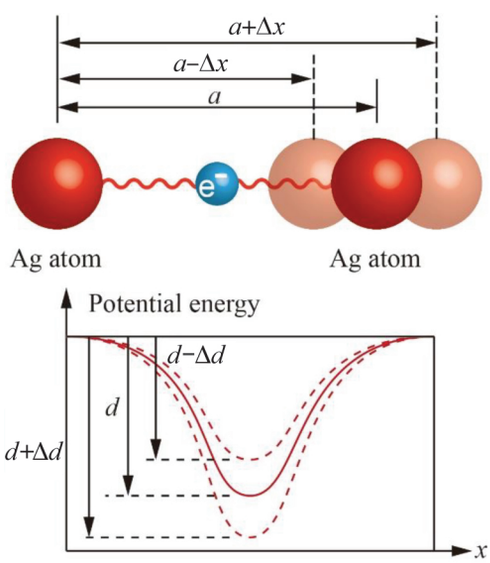

Fig.7 Electron emission model and corresponding qualitative relationship at boundary

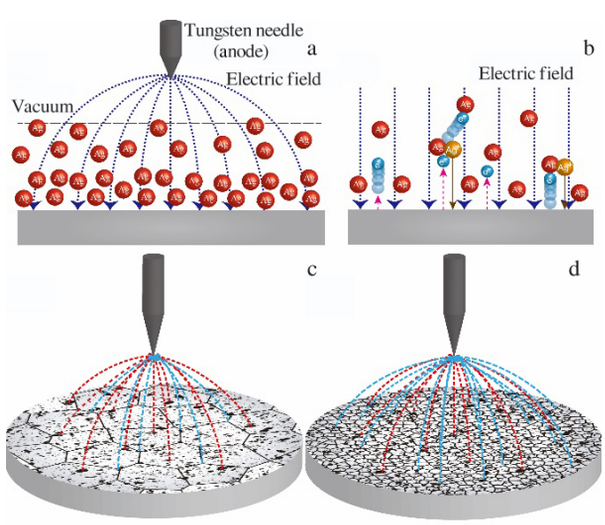

Fig.8 Schematic diagrams of the vapor layer near the metal surface and the distribution of electric field (a), the electron emission and collision with Ag atoms (b), and the emission spots of Ag(72)-4wt% TiB_2 (c) and Ag(0.4)-4wt% TiB_2 (d) contact materials

powders can increase the electron emission spot and current, which further increases the arc duration[22].

The dispersion of electron emission spots can also decrease the energy barrier for arc hop of Ag(0.4)-4wt% TiB_2 contact materials, resulting in the fact that the fine Ag powders can disperse arc. As Ag has a lower work function than TiB_2 does, the arc prefers to generate at the Ag matrix surrounded by the TiB_2 particle due to the higher interface energy between Ag and TiB_2[2]. The arc also prefers to hop to the site with higher Ag vapor content or the electron emission spot. For the Ag(72)-TiB_2 contact materials, it is necessary for arc to hop over a large gap (at least 72 μm), and more serious arc erosion occurs at each site. Hence, the Ag(72)-TiB_2 contact materials have less erosion area and deeper erosion pits. On the contrary, for the Ag(0.4)-TiB_2 contact materials, the arc needs to hop over only a small gap (at least 0.4 μm) to reach the next site. The arc can hop quickly with shorter duration at each site. Therefore, larger erosion area and shallower erosion pit occur on the surface of Ag(0.4)-TiB_2 contact materials.

With the arc erosion circularly proceeding, the repeatable melt and solidification destroy the original microstructure which causes the arc dispersion of Ag(0.4)-TiB_2 contact materials. After the first arc erosion, the distribution of saturation vapor pressure is dominated by the erosion morphologies

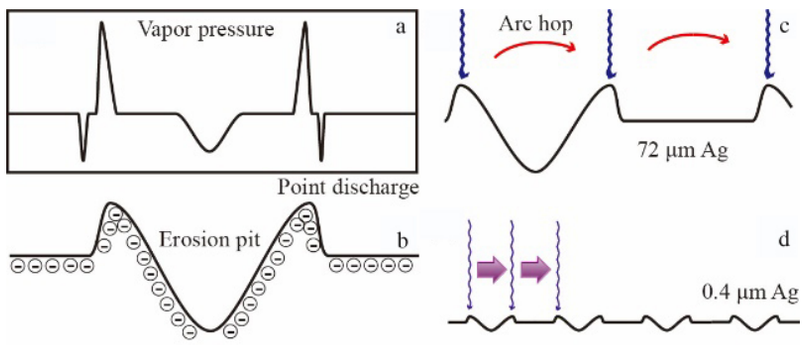

Fig.9 Schematic diagrams of vapor pressure (a) and point discharge (b) of Ag-TiB_2 contact materials and arc hop of Ag(72)-4wt% TiB_2 (c) and Ag(0.4)-4wt% TiB_2 (d) contact materials

rather than the distribution of Ag powders. The distribution of saturation vapor pressure and point discharge at the erosion pit are shown in Fig. 9a and 9b, respectively. Both the point discharge and high saturation vapor pressure exist on the convex with a small curvature radius. Hence, the size and distribution of erosion pit on the eroded surface can influence the arc motion. After the first arc erosion, the erosion pits with different sizes and distributions occur in the Ag-TiB_2 contact materials. For the Ag(72)-TiB_2 contact materials, the deep and concentrated erosion pit occurs with long arc hop distance (Fig. 9c). Hence, the concentrated arc erosion still exists, and the arc has a poor hop ability for the following arc erosion. On the contrary, for the Ag(0.4) -TiB_2 contact materials, the erosion pits are dispersive, and the dispersive arc erosion can still be generated during the following arc erosion (Fig. 9d). In this case, each arc erosion depends on the morphology caused by the last arc erosion. Thus, the Ag(0.4) -TiB_2 contact materials have good arc erosion resistance.

With the evaporation, splash, and flow of the molten Ag, the mass loss is increased gradually, and the fresh Ag layer is exposed accordingly. According to Fig. 8, the new layer with original microstructure can disperse arc as well. Subsequently, the fine Ag powders can maintain the arc dispersion after arc erosion for many times.

3 Conclusions

1) Ag-4wt% TiB_2 contact materials with Ag powder of 0.4 μm have better relative density, electroconductivity, and hardness than those with Ag powder of 72 μm do.

2) Ag-4wt% TiB_2 contact materials with Ag powder of 0.4 μm have longer arc duration with smaller standard deviation than those with Ag powder of 72 μm do. Furthermore, the fine Ag powders are beneficial for the large erosion area, shallow erosion pits, and arc dispersion, thereby resulting in better arc erosion resistance.

3) For the Ag-4wt% TiB_2 contact materials, different distributions of electron emission spot can influence the contact material after arc erosion for the first time. Subsequently, the characteristics of contact materials depend on the morphologies caused by the last arc erosion. Fine Ag powder can maintain the arc dispersion of Ag-4wt% TiB_2 contact materials after arc erosion for 40 times.

References

1 Yang Tianzu, Du Zuojuan, Gu Yingying *et al*. *Transactions of Nonferrous Metals Society of China*[J], 2007, 17: 434

2 Wang Xianhui, Yang Hao, Chen Mei *et al*. *Powder Technology* [J], 2014, 256: 20

3 Li Guijing, Cui Huijie, Chen Jun *et al*. *Journal of Alloys and Compounds*[J], 2017, 696: 1228

4 Wang Jun, Tie Shengnian, Kang Yongqiang *et al*. *Journal of Alloys and Compounds*[J], 2015, 644: 438

5 Mutzel T, Braumann P, Niederreuther R. *Proc 55th IEEE Holm Conf Elect Contacts*[C]. Vancouver: IEEE, 2009: 202

6 Jeannot D, Pinard J, Ramoni P *et al*. *IEEE Transactions on Components Packaging & Manufacturing Technology Part A*[J], 1994, 17(1): 17

7 Wang Xianhui, Li Guijing, Zou Juntao *et al*. *Journal of Composite Materials*[J], 2010, 45(12): 1285

8 Lungu M, Gavriliu S, Canta T *et al*. *Journal of Optoelectronics & Advanced Materials*[J], 2006, 8(2): 576

9 Wang Junbo, Li Yingmin, Wang Yaping *et al*. *Rare Metal Materials and Engineering*[J], 2004, 33(11): 1213 (in Chinese)

10 Xu Aibin, Wang Yaping, Ding Bingjun. *Chinese Journal of Materials Research*[J], 2003, 17(2): 156 (in Chinese)

11 Wang Xianhui, Liang Shuhua, Yang Ping *et al*. *Vacuum*[J], 2009, 83(12): 1475

12 Zhang Miao, Wang Xianhui, Yang Xiaohong *et al*. *Transactions of Nonferrous Metals Society of China*[J], 2016, 26(3): 783

13 Gao Qianwen, Wang Xianhui, Zou Juntao *et al*. *Rare Metal Materials and Engineering*[J], 2017, 46(2): 503 (in Chinese)

14 Qu Jinrong, Hu Mingan, Chen Jingzhong *et al*. *Earth Science*[J], 2005, 30(2): 195 (in Chinese)

15 Feng Yu, Zhang Chengyu, Ding Bingjun. *Rare Metal Materials and Engineering*[J], 2005, 34(9): 1439 (in Chinese)

16 Chen Z K, Sawa K. *IEEE Transactions on Components Packaging & Manufacturing Technology Part A*[J], 1998, 21(2): 310

17 Swingler J, Sumption A. *Rare Metals*[J], 2010, 29(3): 248

18 Swingler J, Mcbride J W. *IEEE Transactions on Components Packaging & Manufacturing Technology Part A*[J], 1996, 19(3): 404
19 Jemaa N B, Doublet L, Jeannot D. *Proc 48th IEEE Holm Conf Elect Contacts*[C]. Orlando: IEEE, 2002: 128
20 Li Hangyu, Wang Xianhui, Guo Xiuhua *et al*. *Materials & Design*[J], 2017, 114: 139
21 Li Hangyu, Wang Xianhui, Liu Yanfeng *et al*. *Vacuum*[J], 2017, 135: 55
22 Smeets R P. *IEEE Transactions on Plasma Science*[J], 1989, 17(2): 303

不同粒度银粉的Ag-TiB_2触头材料电弧侵蚀行为

李航宇[1]，王献辉[1]，高倩雯[1]，梁　燕[1,2]，费　媛[1]
(1. 西安理工大学 陕西省电工材料与熔(浸)渗技术重点实验室，陕西 西安 710048)
(2. 西北有色金属研究院，陕西 西安 710016)

摘　要：采用不同粒度的银粉和放电等离子烧结工艺制备了Ag-4% TiB_2（质量分数，下同）触头材料，测量了Ag-4% TiB_2触头材料的致密度、导电率和硬度，并在真空下对Ag-4% TiB_2触头材料进行了电弧侵蚀实验。采用扫描电子显微镜对Ag-4% TiB_2触头材料电弧侵蚀后的表面形貌进行了表征，采用TDS-2014双通道数字存储示波器记录了燃弧波形，并计算了燃弧时间，对电弧侵蚀机理进行了探讨。结果表明，Ag-4% TiB_2触头材料的致密度、导电率和硬度均随着Ag粒度的降低而增加。另外，采用细银粉制备的Ag-4% TiB_2触头材料具有较长的燃弧时间、较大的侵蚀面积和较浅的蚀坑，表明细小的Ag颗粒有助于电弧分散，能够提高材料的耐电弧侵蚀性能。

关键词：触头材料；Ag-TiB_2；Ag粉粒度；电弧侵蚀

作者简介：李航宇，男，1991年生，博士生，西安理工大学陕西省电工材料与熔（浸）渗技术重点实验室，陕西 西安 710048，E-mail：watcherhyli@163.com